https://doi.org/10.5194/egusphere-2025-6225
Preprint. Discussion started: 18 February 2026

Effect of inlet turbulence on the large eddy simulation of fire plume turbulent characteristics near the ground

Yujia Sun[1], Qing Chen[2], Guanghui Yuan[1]

[1]School of atmospheric physics, Nanjing University of Science and Technology, 210044, Nanjing, China.
[2]College of Mechanical and Electronic Engineering, Nanjing Forestry University, 210037, Nanjing, China.

Correspondence to: Yujia Sun (yujia.sun@nuist.edu.cn)

Abstract. Fire hazard has become a severe threat for ecosystem and urban city. Accurate modelling of fire behaviour and pollutant transport in the atmospheric boundary layer is important for fire risk management. The effect of using turbulent inflow model on simulating fire plume development remains unclear. To understand whether it is important or not for large eddy simulations of fire plume, we performed numerical experiments of fire combustions under uniform and turbulent inflows, and considered two wind velocities, representing weak and moderate conditions respectively. Results show that the assumption of uniform flow does not have significant effect on the mean temperature and velocity fields for weak wind but obvious effect for moderate wind. Turbulent fluctuations of the fire flame indicates that fire plume development modelling is more influenced by the background wind turbulence under relatively larger velocity.

1 Introduction

Fire hazard has become a severe issue in recent years and post significant threat for ecosystem and urban city (Liu et al. 2021). Accurate modelling of fire behaviour and pollutant transport in the atmospheric boundary layer is important for fire risk management (Song et al. 2022; Gajendiran et al. 2024). Due to strong heat released by the fire, the fire plume updraft is dominated by the buoyant force under quiet atmosphere (Maragkos and Merci 2020). Under windy atmosphere, the fire development is influenced by the combined effect of wind inertial and flame buoyance (Pimont et al. 2012). For the large eddy simulation of atmospheric boundary layer (ABL), turbulence must be accurately modelled (Stoll et al. 2020).

Modelling strategy of turbulence for applications related to ABL are extensively investigated. An important component of this modelling is the turbulent inflow condition (Yang et al. 2020). The simplest method is to neglect the velocity fluctuation for the inflow and assumes a uniform velocity profile, which has non-negligible effect on the wind-building interaction modelling (Cheng et al. 2025). Advanced turbulent generation methods have been proposed for the inflow boundary condition, such as the precursor-successor method and the synthetic method. The precursor method is accurate and simple to use but needs more computation load (more time for precursor run and more space requirement for inlet data storage), and the synthetic methods are less computational expensive. There are different kinds of synthetic methods available in

https://doi.org/10.5194/egusphere-2025-6225
Preprint. Discussion started: 18 February 2026

literatures (Melaku and Bitsuamlak 2021). These inflow generation methods are frequently used for building (Melaku and Bitsuamlak 2024) and turbine simulations (Stanislawski et al. 2023). Recently, this kind of inflow turbulence generation model has also been implemented in WRF (Weather Research & Forecasting) for large eddy simulations (Zhong et al. 2021).

Modelling the inflow turbulence is found to have significant effect on the downstream pollutant transport and wake flow (Yang and Sotiropoulos 2019). However, in the modelling of fire plume development, the turbulent inflow condition receives much less attention, although these exist several studies considering turbulent approaching flow. In general, fire releases a large amount of heat in a short time, the turbulent flow near the flame is dominated by the buoyant flow and its associated entrainment flow (Ahmed and Trouvé 2021; Sun et al. 2022). The oscillation of the flame is also mainly controlled by the puffing frequency of the fire plume, which is much less than that of the background wind turbulence. Many studies used a uniform velocity without turbulence or a simplified turbulent method for the approaching flow, which does not represent the true turbulent condition. Eftekharian et al. (Eftekharian et al. 2019, 2020) performed large eddy simulations of wind and fire interactions for different configurations, and used the "2D vortex method" to induce turbulent fluctuations, which was realized by the "turbulentInlet" boundary condition available in OpenFOAM (Open Field Operation And Manipulation) libraries. Edalati-nejad et al. (Edalati-nejad and Ghodrat 2021) also used the random noise method to generate velocity fluctuations for simulations of fires on a sloped terrain. However, they did not discuss the role of this turbulent inflow on the fire heat and flow characteristics. Sun et al. (Sun et al. 2024a, b) used the uniform inflow method for their investigations of fire plume interactions with an idealized building and two-dimensional ridge. This simplified uniform inflow condition may cause errors for pressure coefficient predictions on a building, but how it affects the fire plume interactions with building or ridge were not discovered. Several studies adopted turbulent inflow for their fire modelling (Ong et al. 2022; Wang et al. 2023; Ding et al. 2025) with the precursor method or the synthetic method, but its roles in the fire plume development were not investigated.

From above review, the effect of using turbulent inflow model on simulating fire plume development has not been clearly established, and there is no consensus about its significance. To determine whether it is important for fire plume simulation near the ground, we performed large eddy simulations of fire combustions under uniform and turbulent inflows for two wind velocities, representing weak and moderate wind respectively. Section 2 presents the numerical methods and boundary conditions for the fire combustion modelling and Section 3 provides detailed comparisons of mean temperature and velocity fields and turbulent statistics under different conditions, followed by conclusions and discussions.

2 Methods

https://doi.org/10.5194/egusphere-2025-6225
Preprint. Discussion started: 18 February 2026

2.1 Mathematic formulations and physical models

The fire flame is simulated by a turbulent diffusion combustion model, which considers mass transfer, momentum transfer, species transfer, and energy transfer:

$$\frac{\partial \bar{\rho}}{\partial t}+\frac{\partial \bar{\rho}\tilde{u}_i}{\partial x_i}=0\,, \tag{1}$$

$$\frac{\partial \bar{\rho}\tilde{u}_j}{\partial t}+\frac{\partial \bar{\rho}\tilde{u}_i\tilde{u}_j}{\partial x_i}=-\frac{\partial \bar{p}}{\partial x_j}+\frac{\partial}{\partial x_i}\left(\left(\tilde{\mu}+\mu_t\right)\tilde{S}_{ij}\right)+\bar{\rho}g\,, \tag{2}$$

$$\frac{\partial \bar{\rho}\tilde{Y}_k}{\partial t}+\frac{\partial \bar{\rho}\tilde{u}_i\tilde{Y}_k}{\partial x_i}=\frac{\partial}{\partial x_i}\left(\bar{\rho}\left(D_k+\frac{\nu_{\mathrm{sgs}}}{Sc_t}\right)\frac{\partial \tilde{Y}_k}{\partial x_i}\right)+\overline{\dot{\omega}_k'''}\,, \tag{3}$$

$$\frac{\partial \bar{\rho}\tilde{h}}{\partial t}+\frac{\partial \bar{\rho}\tilde{u}_i\tilde{h}}{\partial x_i}=\frac{\partial}{\partial x_i}\left(\bar{\rho}\left(D_{\mathrm{th}}+\frac{\nu_{\mathrm{sgs}}}{\mathrm{Pr}_t}\right)\frac{\partial \tilde{h}}{\partial x_i}\right)+\overline{\dot{q}_{\mathrm{c}}}\,, \tag{4}$$

where overbars denote density-based variables and tildes denote Favre-based variables. $\bar{\rho}$ is the density, $\tilde{u}$ is the velocity, $\bar{p}$ is the pressure, $\tilde{\mu}$ is the dynamic viscosity, μ_t is the turbulent viscosity, $\tilde{S}_{ij}$ is the shear stress, g is the gravitational force, $\tilde{Y}_k$ is the mass fraction of species k, D_k is the mass diffusion coefficient, Sc_t is the turbulent Schmidt number, ν_{sgs} is the sub-grid scale viscosity, $\overline{\dot{\omega}_k'''}$ is the chemical reaction rate, $\tilde{h}$ is the enthalpy, D_{th} is the thermal diffusion coefficient, Pr_t is the turbulent Prandtl number. The Lewis number is assumed to be unity.

The sub-grid scale turbulent kinetic energy k_{sks} is modelled by a one-eddy equation:

$$\frac{\partial\left(\bar{\rho}k_{\mathrm{sgs}}\right)}{\partial t}+\nabla\cdot\left(\bar{\rho}\tilde{u}k_{\mathrm{sgs}}\right)=\nabla\cdot\left(\left(\mu+\mu_t\right)\nabla k_{\mathrm{sgs}}\right)+P-\bar{\rho}\varepsilon_{\mathrm{sgs}} \tag{5}$$

where μ_t is the turbulent viscosity, and calculated by $\mu_t=\bar{\rho}c_k\Delta\sqrt{k_{\mathrm{sks}}}$.

The flame fuel is assumed to be methane vapor, which flows into the domain through the fuel inlet surface. The combustion occurs immediately once the methane vapor mixes with air under the assumption of eddy dissipation process, which is a widely used model for diffusion flame. Chemical reaction is modelled by one-step global reaction of methane:

$$\mathrm{CH_4+O_2=CO_2+2H_2O} \qquad \text{(R1)} \tag{6}$$

The heat of combustion of the methane is about 5e7 J kg^{-1}, which controls heat release rate of the fuel. Detailed reaction mechanism can be considered for more advanced combustion simulation, but is beyond the purpose of this work.

Figure 1 shows the physical model considered in this work, and the computational domain sizes are 150 m in length, 80 m in wide and 100 m in height. The fire source (methane vapor inlet) is 40 m away from the Inlet surface, which is the wind inlet. The Outlet surface is the exit for the flow. The top surface is set as slip boundary for the velocity and zero gradient for other variables. A Rayleigh damping layer is adopted at the upper 10% of the domain to eliminate the oscillating wave caused by

https://doi.org/10.5194/egusphere-2025-6225
Preprint. Discussion started: 18 February 2026

density variations. To minimize the effect of top boundary on the flame plume development near the ground, the length and height are chosen to make sure the plume mainly exits the domain through the outlet surface. The back and front surface (not labelled) are set as slip for velocity and zero gradient for other variables. Friction at the bottom surface is modelled by a universal law available in OpenFOAM. The fire source is 2 m wide, and discretized in to 8 cells in each direction with mesh size of 0.25 m. To capture temperature and velocity variation near the flame, mesh is refined in this region. The mesh consists of three level grids, as shown in Figure 2. The first level is adopted for the whole domain, the second level is used between (30, 25,0) and (100, 55, 32), and the third level is used between (35, 35,0) and (60, 45,12), which is 25 m long, 10 m wide and 12 m high. This refined mesh leads to a mesh size of 0.25 m in x direction and 0.25m in y direction and 0.06m in z direction. The total number of mesh is about 2.88 million.

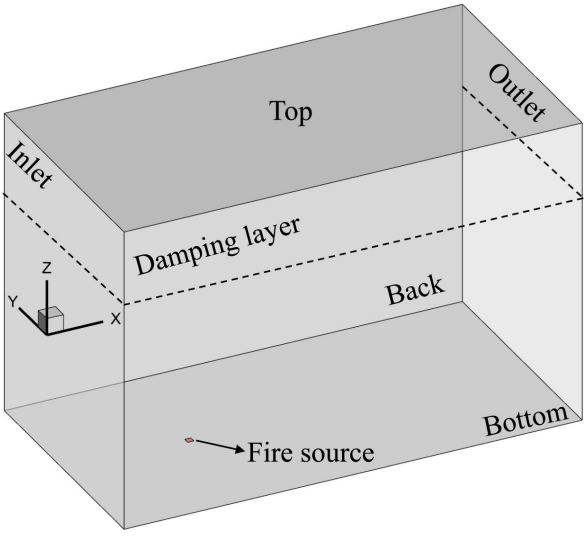

Figure 1 Schematic of physical model and boundary conditions

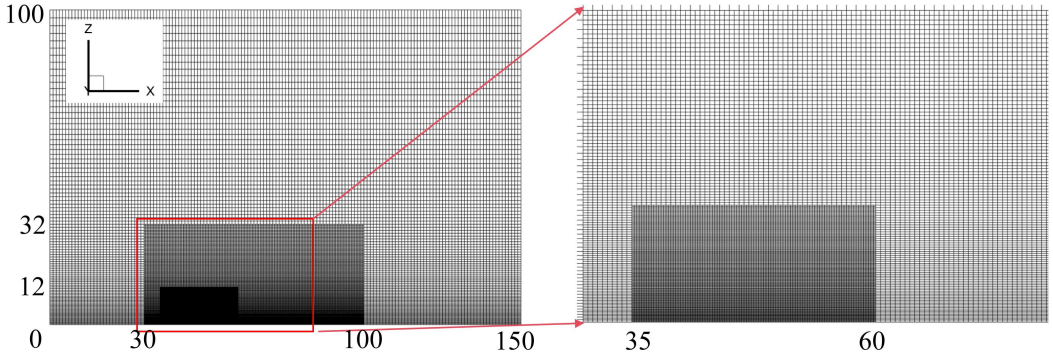

Figure 2 Schematic of refined mesh near the fire source

https://doi.org/10.5194/egusphere-2025-6225
Preprint. Discussion started: 18 February 2026

2.2 Numerical schemes

As for the inlet, two kinds of velocity are considered, a uniform fixed velocity and a turbulent velocity. The uniform fixed velocity uses a power-law profile of $U_0 \cdot (z/10)^{0.12}$, and U_0 is the reference velocity, which is set as 2 m s^{-1} or 5 m s^{-1} in the simulations. This uniform velocity does not induce any turbulence at the inlet, and is sometimes used for the fire modelling in the ABL. The turbulent velocity is generated by the divergence-free spectral representation (DFSR) method, and inputs for this turbulent generation method include mean velocity, turbulent intensities and length scales. The mean velocity profile is same to the uniform case. The turbulent intensities and length scales uses expressions suggested by wind engineering(Yue et al. 2025). In this work, turbulent intensity profile and length scale profile are not varied. We collected the mean velocity profiles and turbulent fluctuations at a location before the fire source. The mean streamwise velocity is shown in Figure 3 ad velocity fluctuations are shown in Figure 4. Because averaging time is short (240s, which is discussed later), these profiles have oscillations. From Figure 3, the mean velocity of the turbulent condition is close to that of the uniform case, but with small deviations from the mean uniform velocity profile due to turbulence. Form Figure 4, velocity fluctuations of the 2 m s^{-1} case are less than 0.03 m^2 s^{-2}, and are less than 0.24 for the 5 m s^{-1} case.

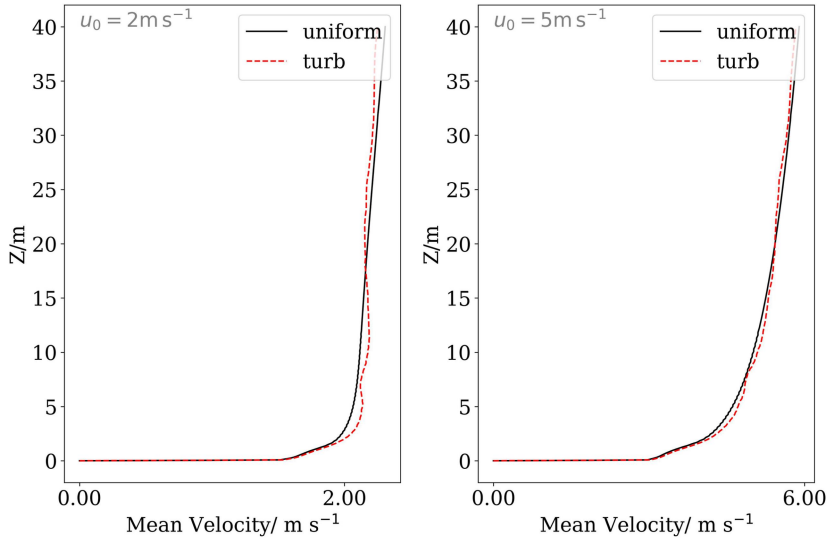

Figure 3 Mean streamwise velocities under different conditions. “uniform” means uniform inflow condition, “turb” means turbulent inflow condition.

https://doi.org/10.5194/egusphere-2025-6225
Preprint. Discussion started: 18 February 2026

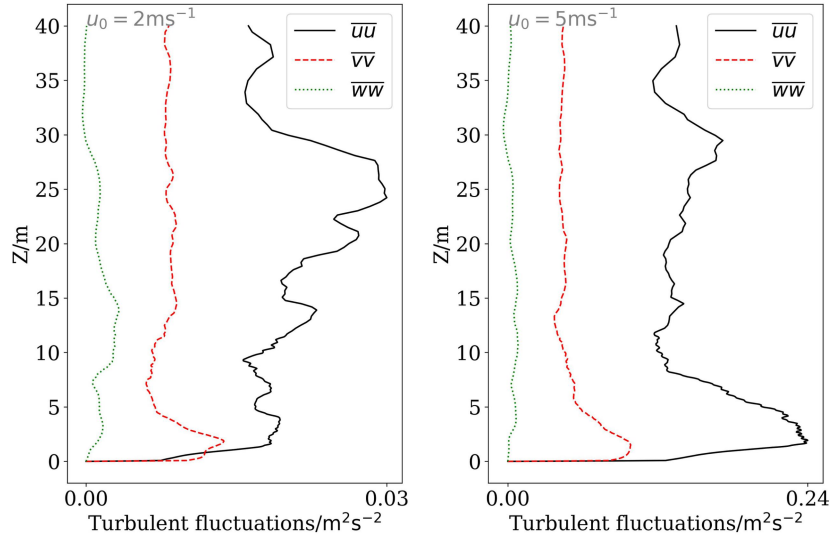

Figure 4 Velocities fluctuations under different conditions.

The Euler method is adopted for the time discretization, and the time step is variable with the maximum Courant number smaller than 0.8. A central differencing scheme with flux limiter is used for the momentum convection term, and total variation diminishing scheme with limiter is applied for the energy and species convection terms, and the species are additionally bounded between 0 and 1. The PIMPLE method (PISO and SIMPLE combined) is used for the pressure-velocity coupling with 3 outer correctors and 2 correctors. Pre-conditioned gradient solver is used for the density and the GAMG (geometric-algebraic multi-grid) with Gauss-Seidel smoother is adopted for pressure equation, while Preconditioned Bi-Conjugate Gradient Stabilized (PBiCGStab) solvers are used for the velocity, energy and species equations.

The simulation process is spin-up for the first 200 s without fuel vapor and combustion. After 200 s, the fuel vapor starts to enter the domain through its inlet and burns immediately when encountering air. Time averaging is activated from 250 s to avoid the effect of initial combustion on the statistic. Total averaging time lasts 240 s, which corresponds to about 3 and 8 flow-through time for wind velocities of 2 m s^{-1}, 5 m s^{-1} respectively. This time window is small for obtaining mean values for the background wind turbulent statistics, but this size is enough for the fire plume turbulent statistics due to its more intermittent flow. Time averaged results for the fire plume are found to be not changing when further increasing time averaging window.

https://doi.org/10.5194/egusphere-2025-6225
Preprint. Discussion started: 18 February 2026

3 Results and Discussions

3.1 Mean velocity and temperature fields

Figure 5 compares mean velocity magnitudes for uniform and turbulent cases at the Y=40 m plane (left column) and X=50 m plane (right column) for U_0=2 m s^{-1}. The velocity distributions at both planes are similar for two cases, but they differ in magnitudes. At the Y middle plane, the maximum velocity occurs near X=43 m or both cases, but the magnitude is higher for turbulent case. At the X=50 m plane, velocity is bimodal due to counter-rotating vortex pairs, and the turbulent case also predicts larger velocity.

Figure 6 compares mean temperature at the Y=40 m plane (left column) and X=50 m plane (right column) for U_0=2 m s^{-1} Temperature distributions are also same for both cases, and the maximum mean temperature can reach about 1600 K. Similar to the velocity fields, temperatures are higher for turbulent cases for both the middle Y plane and X plane.

For the turbulent case, the plume is inclined slightly larger towards downwards, which means that the plume is transported faster at streamwise direction, and this is maybe caused by strengthened streamwise flow or stronger downdraft flow due to turbulence.

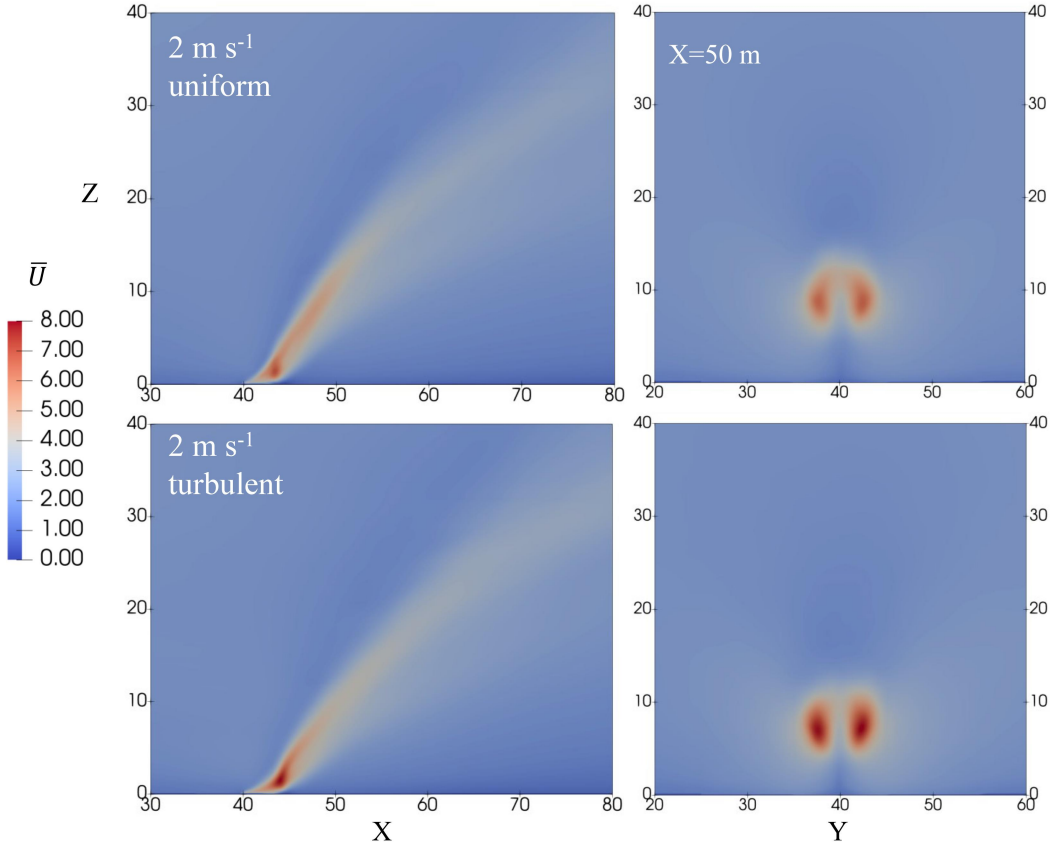

https://doi.org/10.5194/egusphere-2025-6225
Preprint. Discussion started: 18 February 2026

Figure 5 Mean velocity at the Y=40 m plane (left column) and X=50 m plane (right column) for U_0=2 m s^{-1}. First row for uniform condition, and second row for turbulent condition.

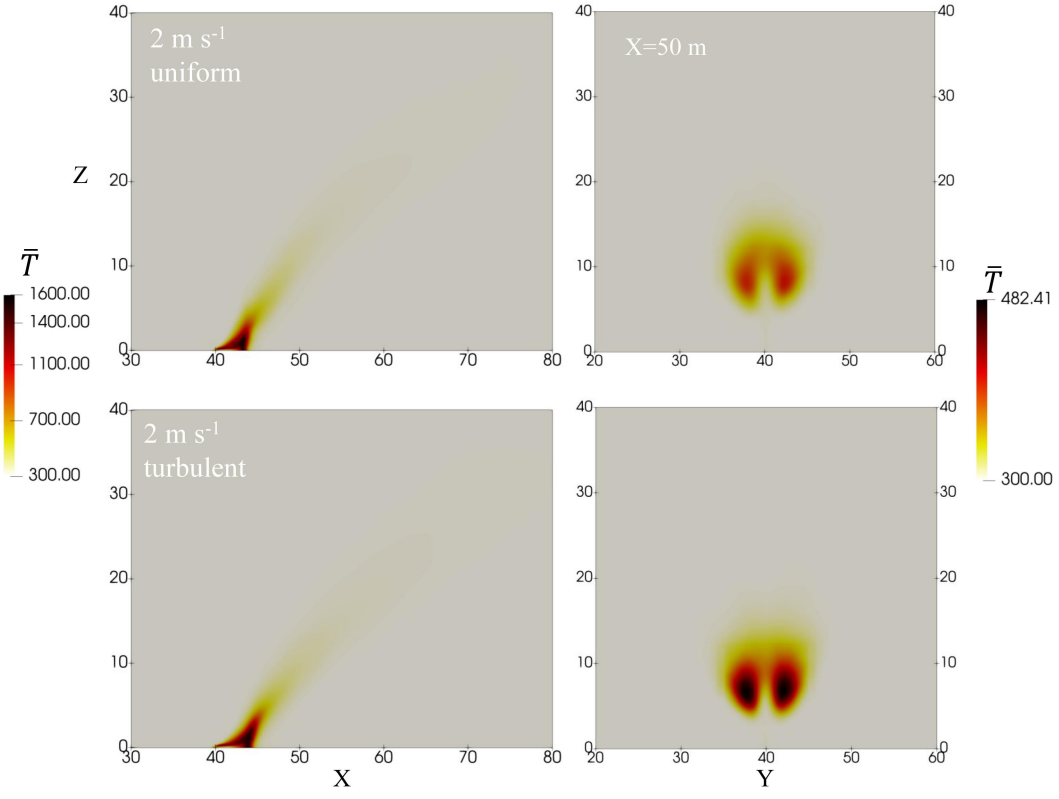

Figure 6 Mean temperature at the Y=40 m plane (left column) and X=50 m plane (right column) for U_0=2 m s^{-1}. First row for uniform condition, and second row for turbulent condition.

Figure 7 compares mean velocity magnitudes for uniform and turbulent cases at the Y=40 m lane (left column) and X=50 m lane (right column) for U_0=5 m s^{-1}. The velocity distributions are similar for two cases at the middle Y plane, but different at the X plane. Due to stronger wind force, plume velocities are much closer to the ground compared to those of 2 m s^{-1} cases. At the Y middle plane, the maximum velocity induced by the fire heat is much higher for the uniform case, and it occurs near X=47 m However, for the turbulent case, the velocity is much smaller and seems more scattered. At the X=50 m plane, velocity is also higher for the uniform case, with a larger velocity gradient in the cores of the plume pairs.

Figure 8 compares mean temperature at the Y=40 m lane (left column) and X=50 m plane (right column) for U_0=5 m s^{-1}. Temperature distributions are also inclined larger as the velocity fields. The maximum temperature of the turbulent case is around 1500 K, but can reach about 1900 K for the uniform case, which is different from 2 m s^{-1} case. For the uniform case, the temperature seems to be accumulated at the rear end of the fuel inlet. This is because the fuel vapor is blown downward

https://doi.org/10.5194/egusphere-2025-6225
Preprint. Discussion started: 18 February 2026

with an almost steady pattern under uniform inflow, and the fuel vapor mixes with oxygen at this location, which supports continuous combustion. However, in the turbulent case, the fuel vapor is transported downward with a varying velocity, so the combustion occurs at a larger region, which can be proved by the broader plume tips (before X=50 m) At the X=50 m plane, we can clearly see that the temperature is much higher for the uniform case, with the maximum value near the bottom of the plume pairs.

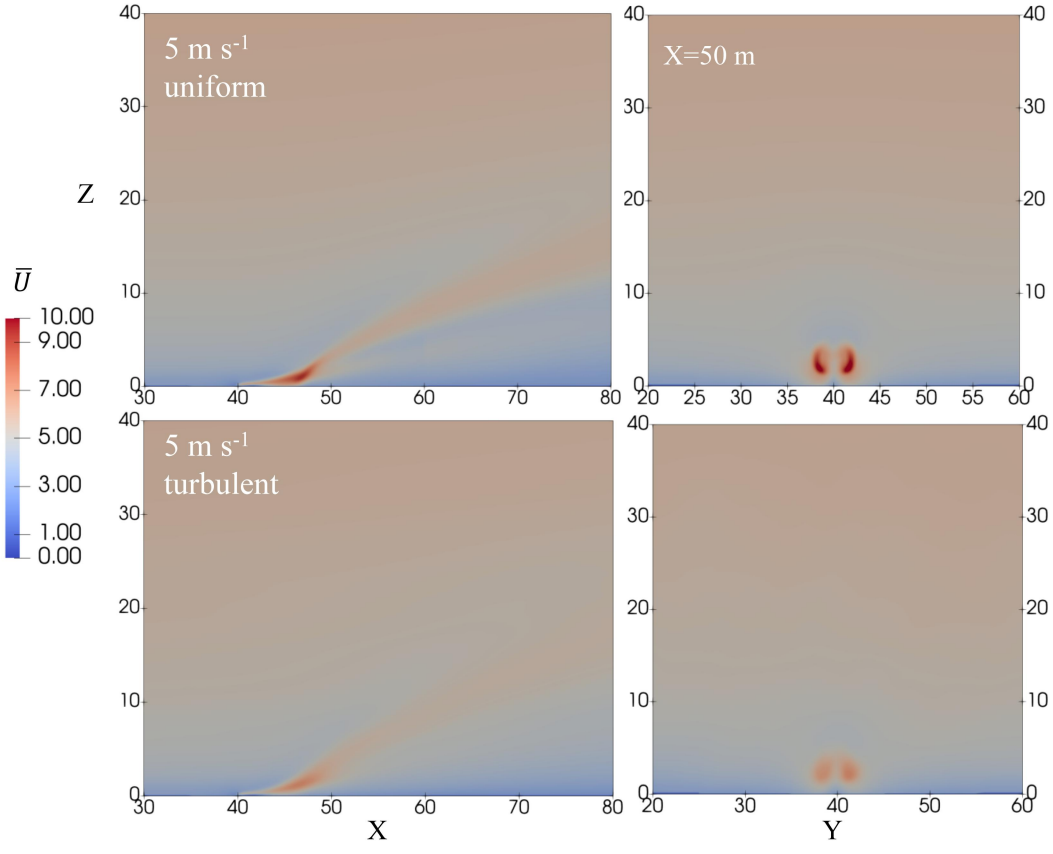

Figure 7 Mean velocity at the Y=40 m plane (left column) and X=50 m plane (right column) for U_0=5 m s^{-1}. First row for uniform condition, and second row for turbulent condition.

https://doi.org/10.5194/egusphere-2025-6225
Preprint. Discussion started: 18 February 2026

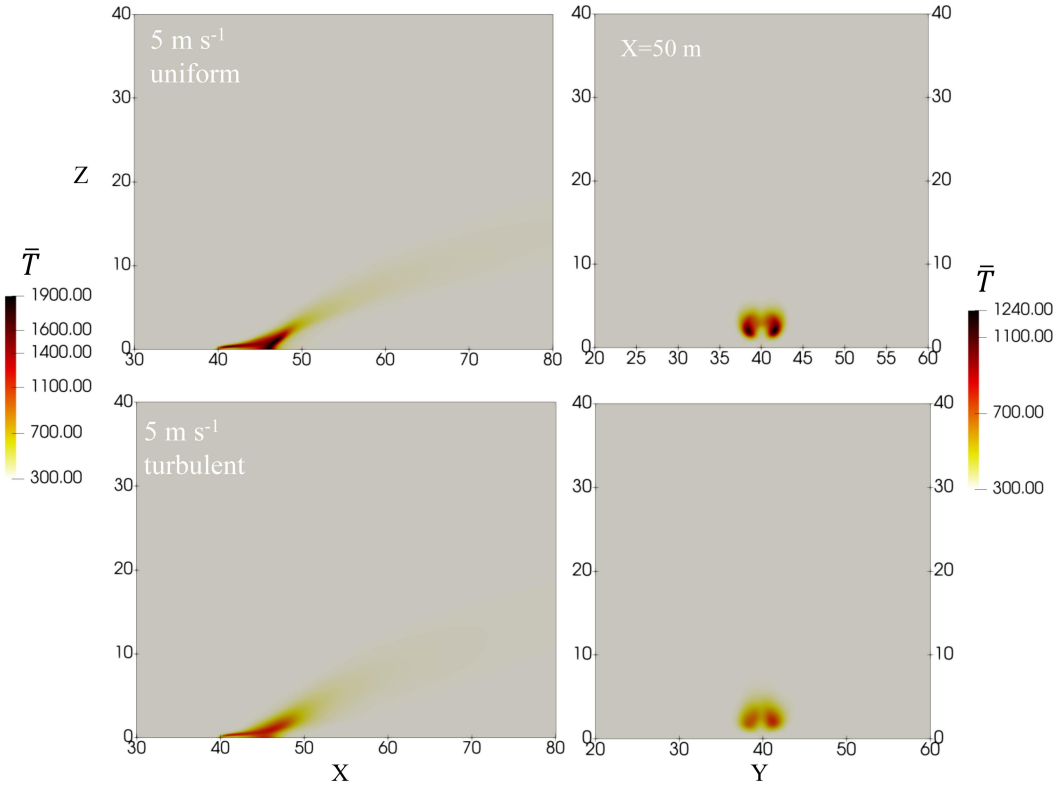

Figure 8 Mean temperature at the Y=40m plane (left column) and X=50m plane (right column) for U_0=5m/s. First row for uniform condition, and second row for turbulent condition.

Figure 9 shows the mean velocity and temperature profiles along height at different x locations for U_0=2 m s^{-1}. At X=43 m to 60 m, it can be clearly seen that the maximum velocity of turbulent case is at lower height compared to that of the uniform case, which means that the plume is more inclined to the surface due to turbulent flow for this wind velocity. However, maximum velocities of two cases are close to each other except for those at X=45 m, which is near the rear end of the fire flame. The dashed red lines seem smoother than the solid black lines, and this means the turbulent inflow does not necessarily lead to more fluctuated flow for this fire plume. At locations further than 60m, velocity of the turbulent case becomes larger than that of the uniform case.

Comparison of temperature profiles shows some differences compared to those of the velocities (figure 10). Temperature of the turbulent case is smaller at X=43 m, but larger at X>=45 m. At X=45 m, the mean temperature of turbulent case is almost two times larger than that of the uniform case. The differences become gradually smaller at further downwards. However, the height of the maximum temperature is smaller for the turbulent case.

https://doi.org/10.5194/egusphere-2025-6225
Preprint. Discussion started: 18 February 2026

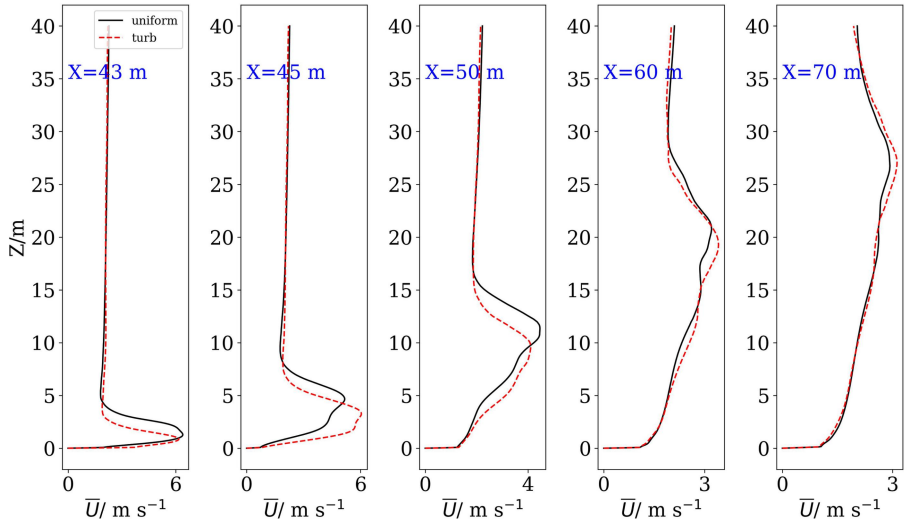

Figure 9 Mean velocity profiles at different x locations for U_0=2 m s^{-1}. The velocities are extracted from the middle Y plane.

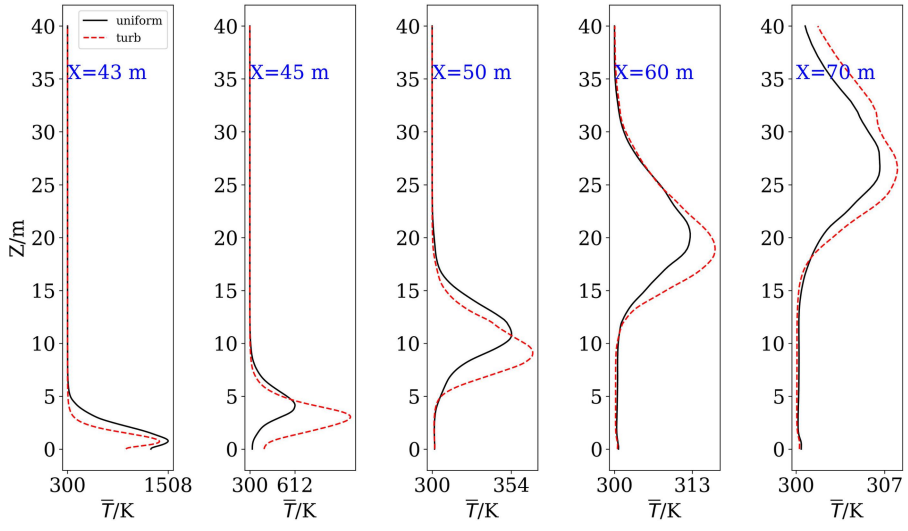

Figure 10 Mean temperature profiles at different X locations for U_0=2 m s^{-1}. The temperatures are extracted from the middle Y plane.

Figure 11 and 12 show the mean velocity and temperature profiles along height at different x locations for U_0=5 m s^{-1}. Velocity of the turbulent case is smaller before X=45 m and become close to that of the uniform case at downstream. Compared to the 2 m s^{-1} condition, a sharp increase of velocity can be observed near the ground surface, which is a consequence of larger inertial under 5 m s^{-1} condition. At further downstream, the velocity profiles of turbulent case are

https://doi.org/10.5194/egusphere-2025-6225
Preprint. Discussion started: 18 February 2026

smoother. Different from the 2 m s^{-1} condition, maximum temperatures of turbulent case are smaller at all X locations, and the maximum difference is located at X=43 m. However, temperature profiles of uniform case have narrower gaussian shapes at X>=50 m. This indicates that the uniform inflow method will decrease the vertical transport of momentum and heat flux.

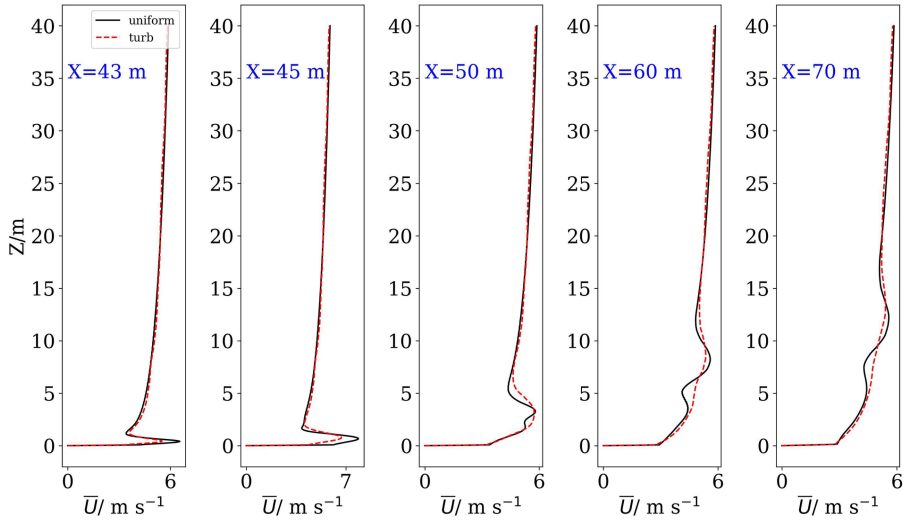

Figure 11 Mean velocity profiles at different x locations for U_0=5 m s^{-1}. The velocities are extracted from the middle Y plane.

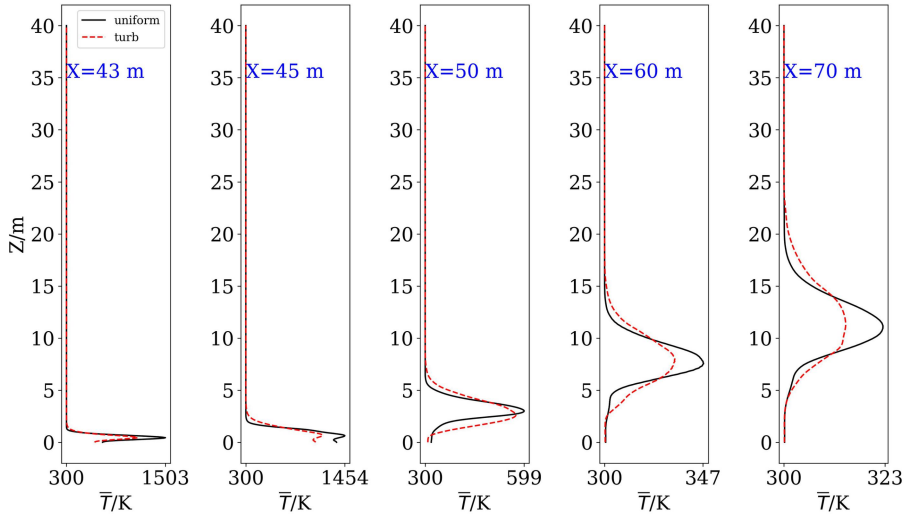

Figure 12 Mean temperature profiles at different x locations for U_0=5 m s^{-1}. The temperatures are extracted from the middle Y plane.

https://doi.org/10.5194/egusphere-2025-6225
Preprint. Discussion started: 18 February 2026

3.2 Turbulent fluctuations

To further reveal the effect of approaching turbulence on the temperature variations, Figure 13 compares root mean square (rms) of temperature fluctuations near the fire flame under different inlet conditions. For both velocities, rms of temperature is more inclined to downstream, similar to the mean temperature and velocity fields. However, there is a significant difference between two velocities. Under 2 m s^{-1} condition, the distributions of rms of temperature are almost same and show a boot-like pattern for uniform or turbulent inflow, with the latter case predicts smaller values. Two feet of the pattern is partially caused by the air entrainment between the interface of the fuel vapor and the environmental air, and the top region is caused by the flame intermittence. Under 5 m s^{-1} condition, patterns of the rms of the temperature are completely different for uniform and turbulent case. For uniform case, the pattern has a narrower region of large rms and the rear foot has much smaller rms compared to that of 2 m s^{-1} condition. This means that temperature is steadier at this region, and this is the reason of high temperature at this region shown in figure 8. For turbulent case, the pattern is completely different, with the high rms regions become wider and the rear foot also become wider. This is maybe caused by the relatively large velocity fluctuations (as in figure 4) for this case, which breaks the steady flame structure that would exist in the uniform case and induce larger streamwise, spanwise and vertical momentum flux.

https://doi.org/10.5194/egusphere-2025-6225
Preprint. Discussion started: 18 February 2026

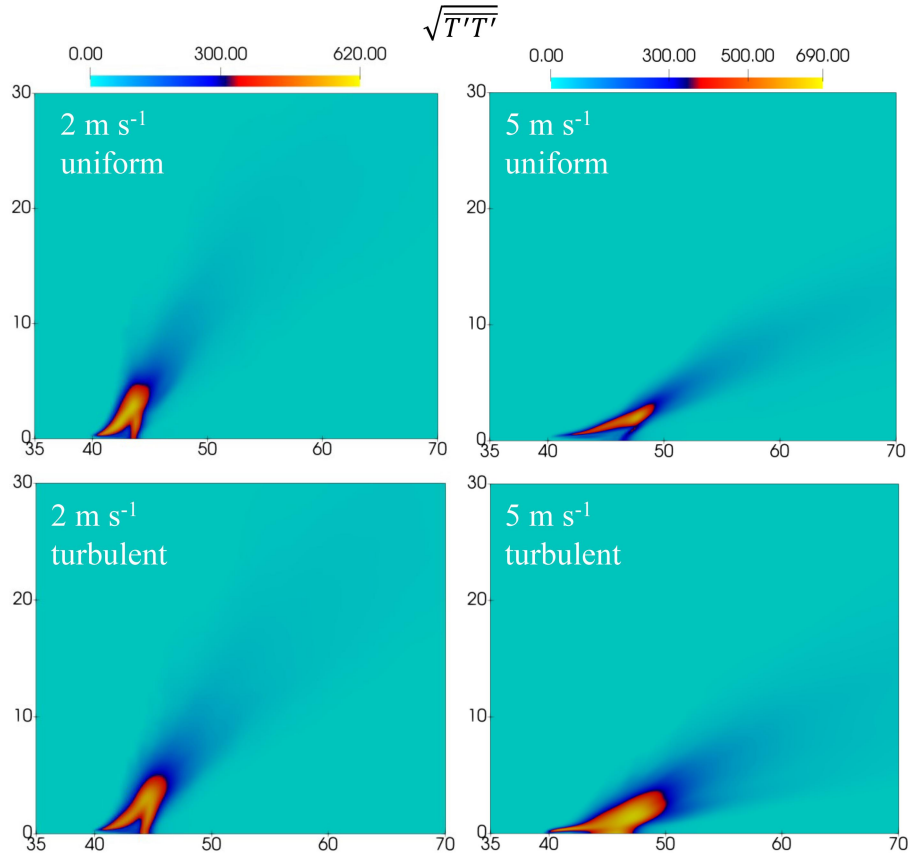

Figure 13 Mean temperature fluctuations near the fire under different inlet conditions.

To show the effect of inlet turbulence on the fire plume turbulent fluctuations, figure 14 compares the streamwise, spanwise and vertical velocity fluctuations under uniform and turbulent cases for U_0=2 m s^{-1}. Maximum values of three components are about 9 m^2 s^{-2}, 3.5 m^2 s^{-2}, and 20 m^2 s^{-2}, with the vertical component has the largest value. Clearly, the turbulent fluctuations at this plane are dominant by the vertical and streamwise components. Three components have very similar structure for uniform and turbulent case, indicating that wind turbulence does not have significant influence on the fire plume turbulent structure, and it is mainly controlled by the buoyant force and mean wind force. However, their distributions are completely different for 5m s^{-1} condition, as shown in figure 15. For this inlet velocity condition, three components of velocity fluctuations are different between the uniform and turbulent cases. For the streamwise component, it is larger for turbulent case, with the maximum value reaches 7 m^2 s^{-2}, while it is only about 3.5 m^2 s^{-2} for the uniform case. Moreover, it encompasses a larger region in turbulent case. For the spanwise component, the difference between the uniform and turbulent case is generally similar to that of the streamwise component. An additional large spanwise fluctuations are observed near the ground at X=47 m for the turbulent case, which means more spanwise momentum flux transport. For the

https://doi.org/10.5194/egusphere-2025-6225
Preprint. Discussion started: 18 February 2026

vertical component, it is smaller for the turbulent case, which may be caused by larger streamwise and spanwise turbulent transport.

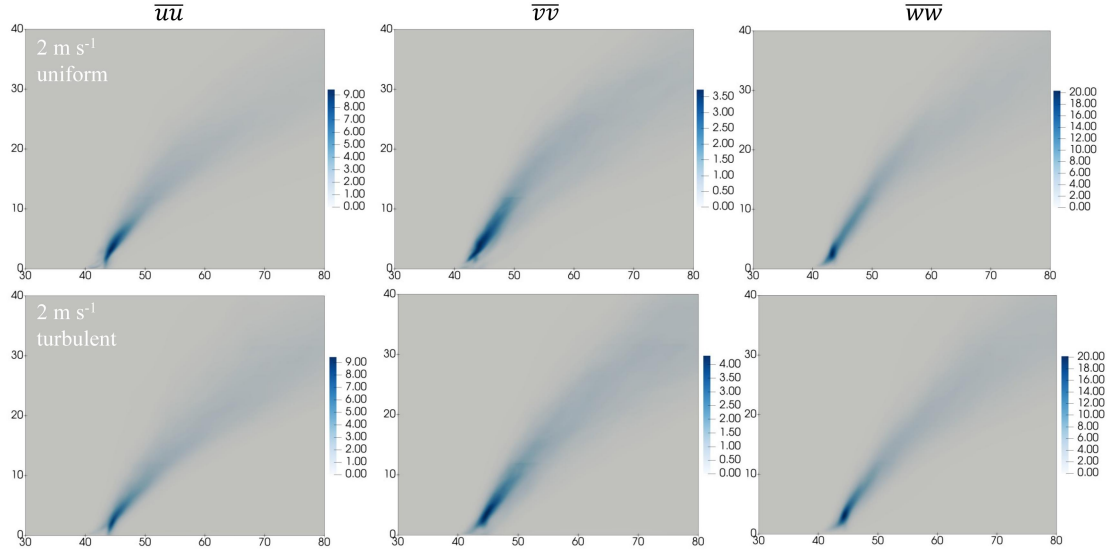

Figure 14 Mean velocity fluctuations of the fire plume for U_0=2m s^{-1}.

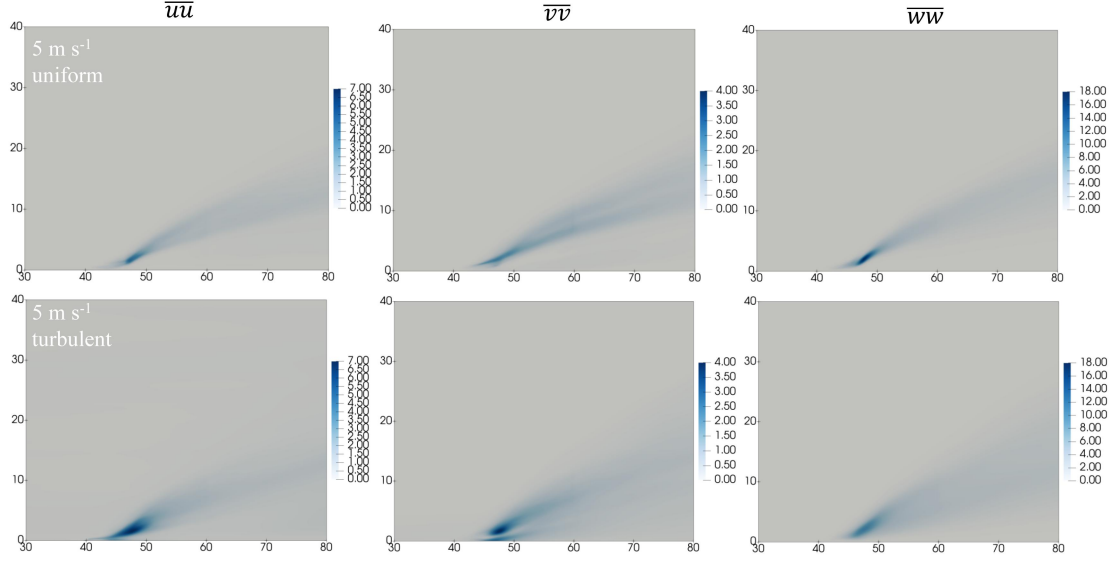

Figure 15 Mean velocity fluctuations of the fire plume for U_0=5m s^{-1}.

https://doi.org/10.5194/egusphere-2025-6225
Preprint. Discussion started: 18 February 2026

Figure 16 and 17 show the normalized turbulent kinetic energy (TKE) profiles along height at different x locations for U_0=2 m s^{-1} and 5 m s^{-1} respectively. The turbulent kinetic energy is calculated as $k = \left(\overline{uu} + \overline{vv} + \overline{ww}\right)/2$. For the 2 m s^{-1} condition, the TKE of the turbulent case is smaller at X=43 m. At X=45 m it is larger for the turbulent case below Z=4 m and larger for the uniform case above Z=4 m. At further downstream, the TKE is always larger for the turbulent case. The TKE become larger at higher locations at further downstream, consistent with the plume rise. For the 5 m s^{-1} condition, the TKE profiles show some different features. Firstly, the fire induced large TKE values are limited to a smaller range below Z=2 m before X= 45 m, which is a consequence of stronger wind force. Secondly, the TKE of the turbulent case is always larger than that of the uniform case except for some heights at downstream (X=60 m and 70 m). This is partially because the approaching flow for this inlet velocity condition has a larger velocity fluctuation along the heights (as shown in figure 4). At downstream, the uniform and turbulent cases predict similar TKE maximum values and corresponding heights. Thirdly, significant differences of TKE maximums between X=43 m and 45 m for the uniform and turbulent cases can be observed near the ground, with the turbulent case having larger values. This large turbulent kinetic energy can considerably alter the flow structure in this region and leads to different mixing and air entrainment here, which eventually cause the different temperature fluctuations (figure 13).

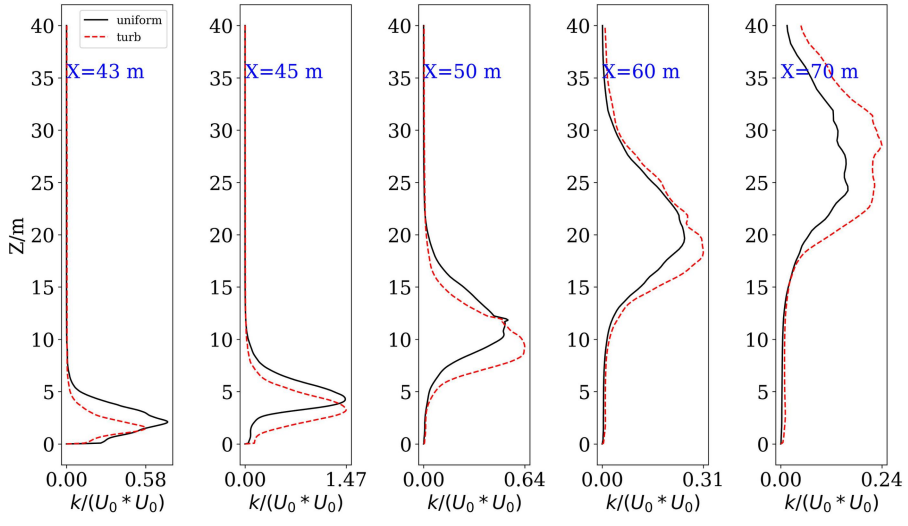

Figure 16 Turbulent kinetic energies (k) at different x locations for U_0=2m s^{-1}. k is extracted from the middle Y plane.

https://doi.org/10.5194/egusphere-2025-6225
Preprint. Discussion started: 18 February 2026

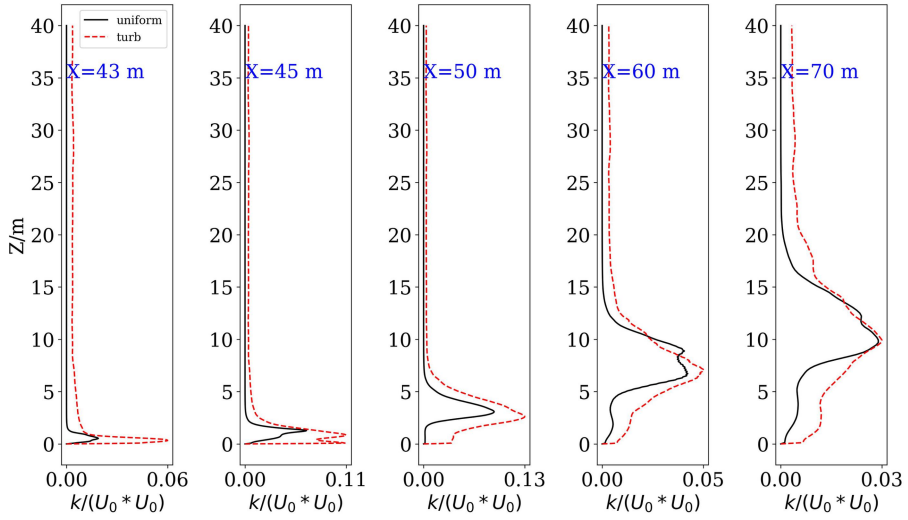

Figure 17 Turbulent kinetic energies (k) at different x locations for U_0=5m s^{-1}. k is extracted from the middle Y plane.

4 Conclusions

The effect of inlet turbulence on the large eddy simulation of fire plume turbulent process is evaluated. This work aims to answer whether the approaching turbulence is important for the LES modeling of fire plume and at what extend it will affect the fire plume characteristics. Its effects are investigated for two background wind conditions, 2 m s^{-1} and 5 m s^{-1} at reference height. The approaching turbulence is generated by a divergence-free spectral representation method for the atmospheric boundary layer. We obtain the following conclusions:

(1) The assumption of uniform flow does not have significant effect on the mean temperature and velocity fields for 2 m s^{-1} case, but the plume height is slightly overestimated. However, it has significant effect for the 5 m s^{-1} case, in which the temperature and velocity is largely overestimated, especially near the rear end of the fire source. The maximum mean temperature difference can reach 300 K, and the mean velocity difference can reach 3 m s^{-1}.

(2) For the mean temperature profiles and mean velocity profiles, the turbulent inflow condition leads to more smooth distributions at downstream, which indicates more momentum transfer in the vertical direction. However, it leads to larger mean temperature and velocity near the flame for the 2 m s^{-1} case, but smaller mean temperature and velocity for the 5 m s^{-1} case.

(3) The assumption of uniform flow shows small effect on the temperature fluctuations near the flame for the 2 m s^{-1} case, but large effect for the 5 m s^{-1} case, in which the turbulent inflow leads to large temperature fluctuations near the rear end of the flame and cause small temperature in this region. This is associated with large turbulent kinetic energies near this region,

https://doi.org/10.5194/egusphere-2025-6225
Preprint. Discussion started: 18 February 2026

which is relatively smaller for the 2 m s^{-1} case. Differences of three components of fluctuations between the unform inflow and turbulent inflow case are also more obvious for the 5 m s^{-1} case. This indicates that fire plume developed is more influenced by the background wind turbulence under relatively large velocity.

This work demonstrates the importance of inlet turbulence on the LES modelling of fire plume development near the ground. There are some limitations for this study. The approaching turbulent intensity is fixed and more investigations can be performed to obtain the dependence of the plume characteristics on the turbulent intensity under different velocities. The work is also limited to a flat surface, and its effect non-flat surface may vary because the terrain induced mechanical turbulence can be quite different. Due to small size of the fire source, the plume rise is not high. For larger fire source, the plume rise may reach hundreds or thousands of meters, its development is further influenced by the stability of the atmosphere, which needs systematic investigations.

Code and data availability

The OpenFOAM (version 1912) software, data and OpenFOAM configurations are available at Zenodo: https://zenodo.org/records/18587305 (Sun 2025). The DFSR code for the generation of turbulent inlet is available at Zenodo: https://zenodo.org/records/18622641 (Sun 2026).

Author contributions

YS performed the simulations, YS and GY analysed the results, YS and QC prepared the figures, and YS prepared the manuscript with contributions from all co-authors.

Competing interests

The authors declare that they have no competing interests.

Financial support

This study is founded by the National Natural Science Foundation of China (No. 42405078).

https://doi.org/10.5194/egusphere-2025-6225
Preprint. Discussion started: 18 February 2026

Review statement

The review statement will be added by Copernicus Publications listing the handling editor as well as all contributing referees according to their status anonymous or identified.

References

Ahmed MM, Trouvé A (2021) Large eddy simulation of the unstable flame structure and gas-to-liquid thermal feedback in a medium-scale methanol pool fire. Combust Flame 225:237–254. https://doi.org/10.1016/j.combustflame.2020.10.055

Cheng Z, Wong JK, Mercan O (2025) Evaluating the wind loads on high-rise buildings of various plan dimensions through numerical simulations. Eng Struct 343:120981. https://doi.org/https://doi.org/10.1016/j.engstruct.2025.120981

Ding B, Hu Y, Cao L, et al (2025) Atmospheric interaction with wildland dual-fires: Flame dynamics and fire-induced flow structures. https://doi.org/10.1063/5.0271530

Edalati-nejad A, Ghodrat M (2021) Numerical Investigation of the Effect of Sloped Terrain on Wind-Driven Surface Fire and Its Impact on Idealized Structures

Eftekharian E, Ghodrat M, He Y, et al (2019) International Journal of Heat and Fluid Flow Numerical analysis of wind velocity effects on fire-wind enhancement. Int J Heat Fluid Flow 80:108471. https://doi.org/10.1016/j.ijheatfluidflow.2019.108471

Eftekharian E, Ghodrat M, He Y, et al (2020) International Journal of Heat and Fluid Flow Correlations for fire-wind enhancement flow characteristics based on LES simulations. Int J Heat Fluid Flow 82:108558. https://doi.org/10.1016/j.ijheatfluidflow.2020.108558

Gajendiran K, Kandasamy S, Narayanan M (2024) Influences of wildfire on the forest ecosystem and climate change: A comprehensive study. Environ Res 240:117537. https://doi.org/https://doi.org/10.1016/j.envres.2023.117537

Liu N, Lei J, Gao W, et al (2021) Combustion dynamics of large-scale wildfires. Proc Combust Inst 38:157–198. https://doi.org/10.1016/j.proci.2020.11.006

Maragkos G, Merci B (2020) On the use of dynamic turbulence modelling in fire applications. Combust Flame 216:9–23. https://doi.org/10.1016/j.combustflame.2020.02.012

Melaku AF, Bitsuamlak GT (2021) A divergence-free inflow turbulence generator using spectral representation method for large-eddy simulation of ABL flows. J Wind Eng Ind Aerodyn 212:104580. https://doi.org/10.1016/j.jweia.2021.104580

Melaku AF, Bitsuamlak GT (2024) Prospect of LES for predicting wind loads and responses of tall buildings: A validation study. J Wind Eng Ind Aerodyn 244:105613. https://doi.org/https://doi.org/10.1016/j.jweia.2023.105613

Ong RH, Patruno L, He Y, et al (2022) Large-eddy simulation of wind-driven flame in the atmospheric boundary layer. Int J Therm Sci 171:107032. https://doi.org/10.1016/j.ijthermalsci.2021.107032

https://doi.org/10.5194/egusphere-2025-6225
Preprint. Discussion started: 18 February 2026

Pimont FA, Dupuy JA, Linn RRB (2012) Coupled slope and wind effects on fire spread with influences of fire size:a numerical study using FIRETEC. Int J Wildl Fire 21:828–842

Song R, Wang T, Han J, et al (2022) Spatial and temporal variation of air pollutant emissions from forest fires in China. Atmos Environ 281:119156. https://doi.org/https://doi.org/10.1016/j.atmosenv.2022.119156

Stanislawski BJ, Thedin R, Sharma A, et al (2023) Effect of the integral length scales of turbulent inflows on wind turbine loads. Renew Energy 217:119218. https://doi.org/https://doi.org/10.1016/j.renene.2023.119218

Stoll R, Gibbs JA, Salesky ST, et al (2020) Large-Eddy Simulation of the Atmospheric Boundary Layer. Boundary-Layer Meteorol 177:541–581. https://doi.org/10.1007/s10546-020-00556-3

Sun Y (2025) effect of inlet turbulent on the LES of fire plume: data [Data set]. https:/ zenodo.org/records/18587305

Sun Y (2026). runtowhere/DFSR: DFSR for LES in OpenFOAM (turbulent_flow). Zenodo. https://doi.org/10.5281/zenodo.18622641

Sun Y, Chen Q, Zheng S, Liu C (2024a) Numerical study of the effects of fire on the flow and wake structures of an idealized building. Phys Fluids 36:. https://doi.org/10.1063/5.0220137

Sun Y, Yu Y, Chen Q, et al (2022) Flow and thermal radiation characteristics of a turbulent flame by large eddy simulation. Phys Fluids 087127: https://doi.org/10.1063/5.0107876

Sun Y, Zheng S, Liu C (2024b) Interaction of the flow and flame dynamics of a line wildfire in the atmospheric wake flow of a ridge. Phys Fluids 36:. https://doi.org/10.1063/5.0203409

Wang Q, Ihme M, Linn RR, et al (2023) A high-resolution large-eddy simulation framework for wildland fire predictions using TensorFlow. Int J Wildl Fire 32:1711–1725. https://doi.org/10.1071/WF22225

Yang Q, Zhou T, Yan B, et al (2020) LES study of turbulent flow fields over hilly terrains — Comparisons of inflow turbulence generation methods and SGS models. J Wind Eng Ind Aerodyn 204:. https://doi.org/10.1016/j.jweia.2020.104230

Yang X, Sotiropoulos F (2019) On the dispersion of contaminants released far upwind of a cubical building for different turbulent inflows. Build Environ 154:324–335. https://doi.org/https://doi.org/10.1016/j.buildenv.2019.02.003

Yue H, Zhang H, Zhu Q, et al (2025) Wake dynamics of a wind turbine under real-time varying inflow turbulence: A coherence mode perspective. Energy Convers Manag 332:119729. https://doi.org/https://doi.org/10.1016/j.enconman.2025.119729

Zhong J, Cai X, Xie ZT (2021) Implementation of a synthetic inflow turbulence generator in idealised WRF v3.6.1 large eddy simulations under neutral atmospheric conditions. Geosci Model Dev 14:323–336. https://doi.org/10.5194/gmd-14-323-2021